

# MC3T3-E1 Osteoprogenitor Cells Systemically Migrate to a Bone Defect and Enhance Bone Healing

Emmanuel Gibon, M.D.,<sup>1,2</sup> Barbara Batke, B.S.,<sup>1</sup> Muhammad Umar Jawad, M.D.,<sup>1</sup> Kate Fritton, B.S.,<sup>1</sup> Allison Rao, B.S.,<sup>1</sup> Zhenyu Yao, M.D.,<sup>1</sup> Sandip Biswal, M.D.,<sup>3</sup> Sanjiv S. Gambhir, M.D., Ph.D.,<sup>3</sup> and Stuart B. Goodman, M.D., Ph.D.<sup>1</sup>

Although iliac crest autologous bone graft remains the gold standard for treatment of bone defects, delayed- and nonunions, and arthrodeses, several alternative strategies have been attempted, including the use of mesenchymal stem cells. Whether cells from the osteoblast lineage demonstrate systemic recruitment to an acute bone defect or fracture, and whether these cells directly participate in bone healing is controversial. This study tests two hypotheses: (1) that exogenous murine MC3T3-E1 osteoprogenitor cells with a high propensity for osteoblast differentiation are able to systemically migrate to a bone defect and (2) that the migrated MC3T3-E1 cells enhance bone healing. Two groups of nude mice were used; a bone defect was drilled in the left femoral shaft in both groups. MC3T3-E1 were used as reporter cells and injected in the left ventricle of the heart, to avoid sequestration in the lungs. Injection of saline served as a control. We used bioluminescence and microCT to assay cell recruitment and bone mineral density (BMD). Immunohistochemical staining was used to confirm the migration of reporter cells. MC3T3-E1 cells were found to systemically migrate to the bone defect. Further, BMD at the defect was significantly increased when cells were injected. Systemic cell therapy using osteoprogenitor cells may be a potential strategy to enhance bone healing.

## Introduction

**H**EALING OF FRACTURES and nonunions, bone defects, spine fusions, and joint arthrodeses is a complex process that demands robust bone healing for restoration of function. Iliac crest autologous bone graft (ICAG) to the local site remains the gold standard for treatment. Newer methods to facilitate bone healing include biological methods<sup>1</sup> (e.g., allograft bone, bone marrow aspirate, demineralized bone matrix, bone morphogenic proteins [BMPs], collagen carriers etc.), mechanical loading protocols, local biophysical/electrical methods (e.g., electrical stimulation and ultrasound), and combined methods. Although bone grafting is the most common treatment for bone repair with over 600,000 procedures—including 200,000 autologous bone grafts<sup>2</sup>—annually performed in the United States,<sup>3</sup> several complications have been reported with autologous bone grafts. Indeed, previous studies<sup>2,4</sup> have shown major complications (e.g., deep infection, chronic severe pain) ranging from 2.4% to 8.6% and minor complications (e.g., hematoma, chronic mild pain) around 20%. In light of these data, a safe and effective method to obtain bone repair without using an ICAG is a current challenge. Indirect healing which requires

both endochondral and intramembranous processes is the most common form of bone healing<sup>5</sup>; in addition to an adequate blood supply and the presence of growth factors and cytokines, bone healing requires osteoprogenitor cell recruitment.<sup>6</sup> Mesenchymal stem cells (MSCs) and osteoprogenitors must proliferate and differentiate into matrix producing osteoblasts. MSCs reside within the surrounding soft tissues (periosteum and muscle), bone marrow, trabecular bone, synovium, and synovial fluid<sup>7,8</sup> and several studies have suggested that MSCs are able to migrate from a remote site to the injury site.<sup>9,10</sup> MSCs and osteoprogenitor cells also circulate in the bloodstream.<sup>11–13</sup> Among this population, Matsumoto *et al.*<sup>13</sup> have shown that more than half of these osteoprogenitors express the CXCR4 receptor, which is markedly involved in osteogenic cell recruitment through the stromal cell-derived factor-1/CXCR4 axis.<sup>14</sup> This finding has been well illustrated by Shinohara *et al.*<sup>15</sup> using an interesting mouse model of parabiosis surgery, establishing a strong relationship between fracture healing and systemic recruitment of MSCs. High levels of SDF-1 (also called CXCL-12) have been reported in fracture supernatants.<sup>16</sup> BMPs are secreted by MSCs in the first 24 h of bone healing.<sup>7</sup> Akman *et al.* highlighted an increase of osteocalcin

<sup>1</sup>Department of Orthopaedic Surgery, Stanford University School of Medicine, Stanford, California.

<sup>2</sup>Department of Orthopaedic Surgery, Bichat Teaching Hospital, Paris School of Medicine, Paris, France.

<sup>3</sup>Department of Radiology, Stanford University School of Medicine, Stanford, California.

and alkaline phosphatase activity when MC3T3-E1 cells (a C57BL murine osteoprogenitor cell line with a high propensity for osteoblast differentiation<sup>17-19</sup>) were cultured with BMP-6-loaded chitosan scaffolds.<sup>20</sup> Further, MC3T3-E1 cells also promote osteoblast cell attachment secreting the C-terminal pro-peptide of type I collagen, as shown by Mizuno *et al.*<sup>21</sup>

The present study was designed to test whether healing of a bone defect involves the systemic recruitment of osteoprogenitor cells. We hypothesized that MC3T3-E1 osteoprogenitor cells can migrate from a remote site of injection to a defect to enhance bone healing. We used a murine non-critical size defect model to primarily study the biology of cellular homing to a bone defect, without confounding mechanical variables. The model provides a surrogate for examining potential applications of systemic cell homing to facilitate bone healing.

## Materials and Methods

### Animals and experimental design

Ten, 12-week-old nude mice nu/nu (Charles River Laboratory, Inc.) were housed and fed in our Animal Facility. The experimental design was approved by the Institutional Administration Panel for Laboratory Animal Care (APLAC number 9943). We strictly followed university guidelines for care and use of laboratory animals. Animals were divided into two groups. Both groups had a surgical defect created in the left femur (see below); Group 1 animals ( $n=5$ ) were injected with  $5 \times 10^6$  MC3T3-E1 subclone 14 cells through a left intracardiac injection and Group 2 animals ( $n=5$ ) were injected with sterile saline solution also through an intracardiac injection. Both of these injections were performed the day after surgery in which a unilateral midshaft femoral drill hole was performed (see below). The animals underwent microCT 1 day before cell injection and at day 14. Bioluminescence was performed at day 0, right after cell injection and at days 1, 2, 4, 6, 8, 10, and 14. All animals were euthanized after final imaging and their femurs were harvested for histomorphometry.

### Surgery

The surgical procedure was performed at day -1, that is, 1 day before subsequent intracardiac osteoprogenitor cell injection (day 0). All animals received an injection of buprenorphine (0.1 mg/kg; Ben Venue Laboratories), subcutaneously before the procedure. Animals were anesthetized with 3% isoflurane in 100% oxygen at a flow rate of 1 L/min and were operated on a warm small animal surgery station. Using a sterile technique, a lateral approach to the left femur was used, the quadriceps was retracted anteriorly, then the femoral shaft was identified under the vastus lateralis. A unicortical lateral bone defect near the middle of the femoral shaft was made using a 0.7 mm drill. Loose bone debris was washed with sterile saline solution. The skin was repaired with 5.0 resorbable sutures. We checked the animals each day postoperatively for general health and activity.

### Cells

We used murine MC3T3-E1 subclone 14 osteoprogenitor cells (American Type Culture Collection) transfected with the

lentivirus vector to express the bioluminescent optical reporter gene firefly luciferase (*fluc*) and a red fluorescent reporter gene (*tomato*). The cell line was grown and maintained in nonosteogenic media in ascorbic acid-free alpha minimum essential medium A10490 (Invitrogen-Gibco)+10% fetal bovine serum (Invitrogen-Gibco)+1% antibiotic-antimycotic (Invitrogen-Gibco). Each mouse within Group 1 received  $5 \times 10^6$  cells suspended in 0.1 mL phosphate-buffered saline with 30 units/mL heparin through an intracardiac injection in the left ventricle.<sup>22,23</sup>

### Imaging

The imaging was performed in the Small Animal Imaging Facility at Stanford University (Clark Center). A microCT scan was performed immediately after surgery (day -1) and at day 7 and 14 to detect changes in bone mineral density (BMD). At day 14, we euthanized the animals, and then microCT was performed again.

The algorithm used to calculate the BMD in MicroView (GE medical Systems) depends on the calibration of the scanner using the phantom provided with the system. During calibration, a region of interest (ROI) within air, water, and SB3 (a bone mimicking material) are obtained within the phantom. The air and water values are used to convert the raw data, which are acquired with arbitrary units, to Hounsfield units (HU) by scaling the air to -1000 and the water to 0. The system then determines an HU value for bone based on an extrapolation from these air and water HU values.

During BMD calculation, the HU value for a voxel with the same grayscale value as the SB3 is converted to the mass of mineral associated with that grayscale value. This is essentially a virtual ashing process. This mathematical correlation is based on a linear relationship between water (0 mg/cc of mineral) and the bone HU calibration value (1073 mg/cc of mineral). The mineral contents of voxels with other grayscale values are then determined based on interpolation (if the value is between the values of the water and bone HU from the calibration) or extrapolation (if the value is outside of the range between air and water). The end result of this calculation is a measured amount of mineral mass. The mineral mass is then divided by a volume to obtain the density.

Anesthesia was maintained by mask inhalation of isoflurane and animals were placed in the ventral position in the device, eXplore RS microCT scanner (GE medical Systems) with 49  $\mu$ m resolution during 8 min. The phantom was placed in the field of view of the ROI (the femur).<sup>24</sup> Irradiation was 19.2 Rads per mouse and per microCT. Before the procedure, scout images were made to confirm that both femurs were entirely scanned. After scanning, we used the eXplore Evolver software (GE medical Systems) for acquisition and eXplore Reconstruction interface software for reconstruction. For BMD assessment we used the MicroView software (GE medical Systems) and a 3D ROI was created (4  $\times$  3  $\times$  3 mm) centered on the defect for the left femur and at the same level for the right femur.

For bioluminescence, we used an *in vivo* imaging system employing a cooled device camera (Caliper LifeScience). Animals were anesthetized with 3% isoflurane during the process. We performed the bioluminescence with 3 mg/

mouse of Luciferase substrate D-Luciferin (Biosynth International), intraperitoneally administered. Five minutes later, images were taken of the whole mouse. For analysis, we drew uniformly sized ROI (1.2×0.5 cm) at the level of the middle third of the femur where the defect was drilled, for each femur. The data was collected and expressed as photon/second/cm<sup>2</sup>/steradian (p/s/cm<sup>2</sup>/sr).

*Histology and immunohistochemistry*

After imaging, all animals were euthanized using both CO<sub>2</sub> inhalation and cervical dislocation. The femora were then collected from the animals (20 femora). Femora were decalcified using paraformaldehyde for 3 days and then using ethylenediaminetetraacetic acid for 2 days twice. Frozen sections of 8 μm were cut using a cryostat (Cambridge Instruments) to include the middle third of the femora, where the defect was previously made. The sections collected were used for immunostaining. Mouse anti-luciferase (Santa Cruz Biotechnology) was used to detect the reporter cells. The secondary antibody used for immunofluorescence was goat antimouse IgG conjugated with Alexa Fluor 488 (Invitrogen). DAPI (Invitrogen) was used to stain nuclei.

We also performed staining with hematoxylin and eosin (H&E) (Sigma) on cut histological sections, for general histomorphological analysis.

*Statistical analysis*

Bioluminescence data (ratio of operated divided by non-operated femora within ROI) and microCT data (BMD) were analyzed by the nonparametric Mann–Whitney U tests (two-tailed) between comparable paired groups (statistiXL Software).

**Results**

Successful MC3T3 intracardiac injection was confirmed by bioluminescence immediately after cell injection: cells were diffusely spread throughout the entire body or slightly con-

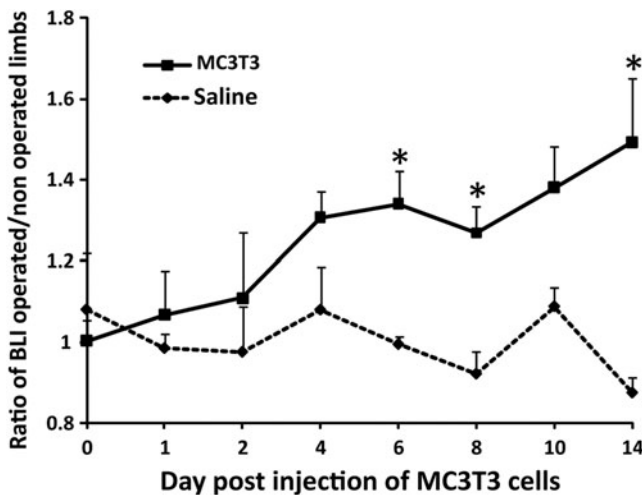


**FIG. 1.** MC3T3 cells injected into the left ventricle have systemically migrated to a bone defect drilled in the left femur. Ratio of bioluminescence signal from operated femora divided by nonoperated femora from day 0 to 14. \**p* < 0.05.

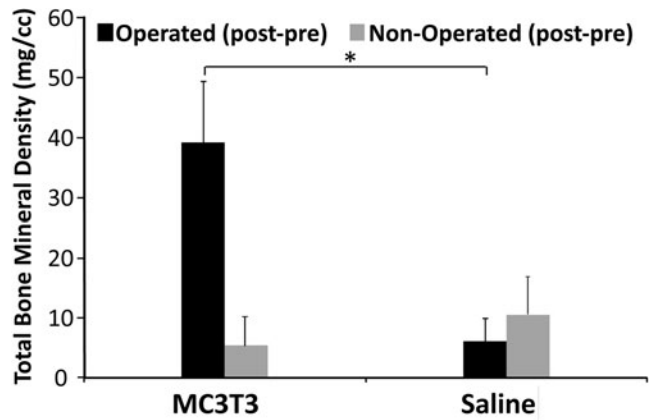


**FIG. 2.** Bone mineral density analysis. Bone density of the callus is significantly increased when mice were injected with MC3T3-E1 cells, compared with control injection of saline. Total bone mineral density (post–pre values). \**p* < 0.05.

centrated in the lungs. Reporter MC3T3 cells injected into the left ventricle were systemically recruited toward the bone defect in the left femur. In Group 1, we observed a significant increase in systemic migration of MC3T3 cells at day 6, 8, and 14. At day 14, the ratio of bioluminescence was 1.49±0.15 for Group 1 receiving MC3T3 cells whereas it was 0.87±0.03 for Group 2 receiving a control injection (*p* = 0.008) (Fig. 1).

microCT analysis confirmed that systemic trafficking of MC3T3 cells enhanced bone defect healing. Total bone mineral density (TBMD) was significantly increased for Group 1 (receiving MC3T3 cells) compared with Group 2 (receiving a saline injection) at day 14. After normalization (post minus pre values), the TBMD was 39.11±10.26 for Group 1 versus 6.07±3.89 for Group 2 (*p* = 0.016) (Fig. 2). Size of the callus was markedly increased at day 14 for Group 1 in the coronal view, compared with Group 2 (Fig. 3).

H&E-stained sections and immunohistochemistry confirmed the migration of reporter cells within the bone defect. With a 5× magnification, H&E staining showed a dramatically smaller size callus for Group 2 whereas the callus was much larger and extensive for Group 1 (Fig. 4A). Immunohistochemistry confirmed the results obtained by bioluminescence, specifically the systemic migration of reporter cells to the callus for Group 1 (Fig. 5).

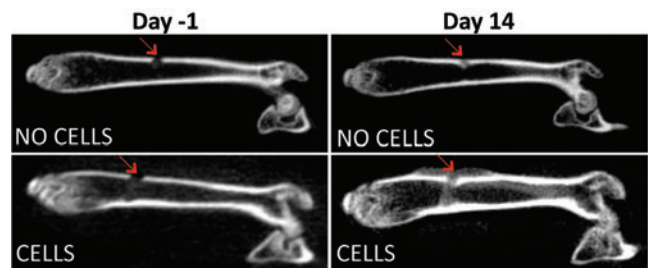


**FIG. 3.** Coronal view of reconstructed left femora. CT performed 1 day before cell injection and at day 14. The size of the callus (red arrows) is increased when mice were injected with reporter cells as opposed to saline alone. Color images available online at [www.liebertonline.com/tea](http://www.liebertonline.com/tea)



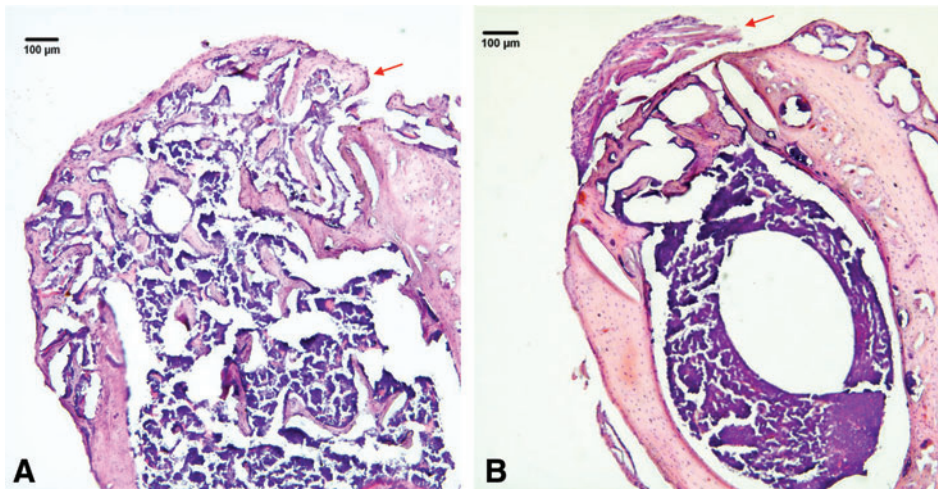


**FIG. 4.** Hematoxylin and eosin-stained sections from frozen, decalcified femora from Group 1 (A) with intracardiac osteoprogenitor cell injection, and Group 2 (B) without cell injection. Note the abundant callus (red arrows) over the cortical defect in Group 1. Plump osteoblasts surround the new woven bone. Original magnification:  $\times 50$ . Color images available online at [www.liebertonline.com/tea](http://www.liebertonline.com/tea)

## Discussion

Our aim was to demonstrate the systemic migration of pre-osteoblasts to a femoral bone defect and to show an acceleration of bone healing. We conclude that MC3T3-E1 osteoprogenitor cells systemically injected are able to localize to a remote bone defect, differentiate into mature osteoblasts, and enhance bone healing, resulting in a larger bony callus. In our study we used nude mice, which are known to have a deficient immune system. These mice were chosen to facilitate bioluminescence of the injected MC3T3-E1 osteoprogenitor cells. However, the deficient immune system in the nude mice may have also facilitated more successful cellular engraftment than would normally be clinically seen. However, our results regarding the sequence of bone healing are consistent with a previous study which used immune-competent non-nude C57BL/6 mice.<sup>25</sup>

Although several studies have suggested systemic recruitment of MSCs using an animal model of fracture or bone defect,<sup>9,10,26,27</sup> little is known about the ability of osteoprogenitor cells to localize to a bone defect from a remote site. Granero Molto *et al.*<sup>9</sup> have shown the ability of non-differentiated MSCs to migrate to a bone defect and highlighted CXCR4 as a critical receptor. Shen *et al.*<sup>27</sup> have demonstrated accelerated bone healing using a stabilized murine femur fracture model with added insulin growth factor-1 (IGF-1) transduced MSCs. Thus, the ability of MSCs to home to a fracture and enhance bone healing has been established. In our current study, we used osteoprogenitors to ascertain whether more differentiated cells are able to systemically migrate to a bone defect. The behavior of early-differentiated bone lineage cells such as MC3T3-E1 osteoprogenitor cells (but not fully mature osteoblasts) is relevant to bone healing. For example, Hernigou *et al.* showed that

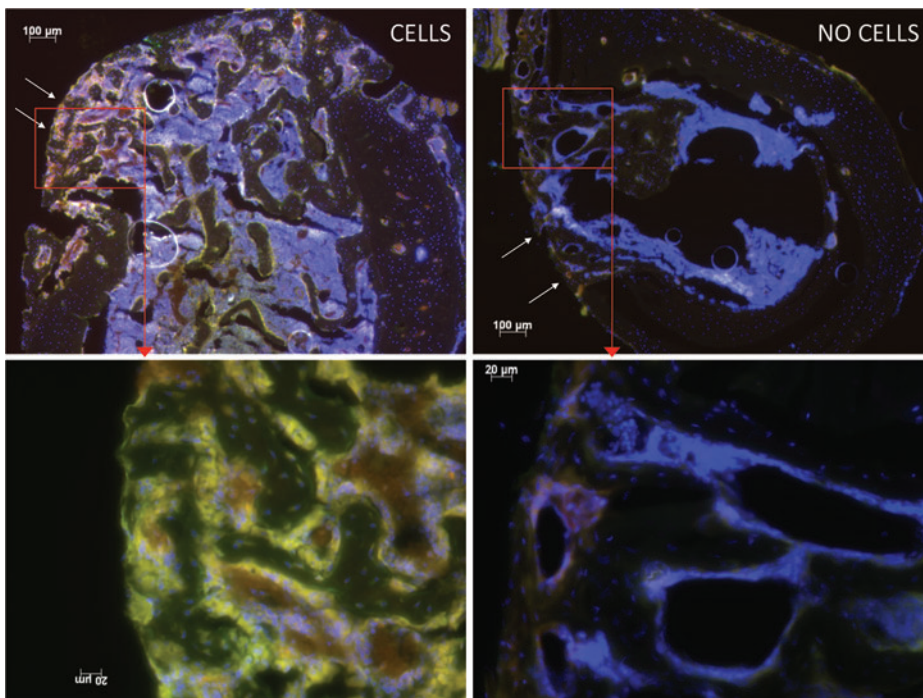


**FIG. 5.** Immunohistochemistry for Group 1 (left column) and Group 2 (right column). The bone defect is marked with arrows. Note that MC3T3-E1 reporter cells (yellow stain) have systemically migrated to the bone defect and produced a large amount of callus. Original magnification:  $\times 50$  (upper line) and  $\times 200$  (lower line). Color images available online at [www.liebertonline.com/tea](http://www.liebertonline.com/tea)

bone marrow aspirates from the iliac crest have a combination of MSCs, fibroblasts, osteoprogenitors, and mature osteoblasts.<sup>28,29</sup> Our study strongly highlights the fact that osteoprogenitors are involved in, and enhance bone defect healing.

MC3T3-E1 cells are a clonal murine cell line of immature osteoblasts derived from mice.<sup>18</sup> In our study, we used the subclone 14 which has been shown to produce a well-mineralized extracellular matrix (ECM) and express osteoblast markers (e.g., osteocalcin, bone sialoprotein, osteoblast-specific factor 2).<sup>17</sup> After bone injury, the initial pro-inflammatory response involves release of numerous factors including BMPs by pro-inflammatory cells.<sup>6,30,31</sup> RbBMP-7 has been shown to enhance the chemotactic recruitment of MC3T3-E1 cells.<sup>32</sup> Kumagai *et al.*<sup>25</sup> used a parabiosis model with GFP transgenic mice to show that the contribution of circulating cells to fracture callus peaks at 2 weeks. We chose to inject the osteoprogenitor cells 24 h after the bone defect was created for cellular migration to be synchronized with the tumor necrosis factor- $\alpha$  (TNF- $\alpha$ ) peak at 24 h.<sup>6</sup> TNF- $\alpha$  has been shown to induce recruitment of cells with osteogenic potential<sup>16,33</sup> and to induce osteogenic differentiation. Moreover, among the major signaling molecules involved in bone repair, IGF-I has autocrine and paracrine effects, and is released by bone matrix, osteoblasts, and chondrocytes during the bone healing process.<sup>7,34</sup> Kim *et al.* have shown a marked relationship between IGF-I and osteoblast function. When MC3T3-E1 cells were cultured with IGF-I plus IGF-binding protein-5, the cells exhibited an increase in ECM proteins synthesis, osteopontin, and thrombospondin-I, which ultimately stimulated the growth of osteoblasts through ERK1/2 phosphorylation.<sup>35</sup>

MC3T3-E1 cells, first described by Sudo *et al.*<sup>36</sup> in 1983, have a fibroblastic shape and their size is about 20–50  $\mu\text{m}$  in diameter. In our study we injected  $5 \times 10^6$  cells into each mouse. Such a large quantity of cells cannot be easily injected through the tail vein due technical reasons. Further these large cells undergo pulmonary sequestration. Therefore, we decided to use systemic delivery using an intracardiac injection into the left ventricle under general anesthesia. To minimize cardiac injury, we used a 30½-gauge needle that allowed us to inject the cells into the left ventricle with minor adverse effects to the surrounding tissues. The presence of bright red oxygenated blood pulsating in the syringe indicated correct placement of the needle and preceded the injection of cells slowly over 20 to 40 s.

## Conclusion

In the presence of a bone defect, MC3T3-E1 osteoprogenitor cells systemically migrated, accelerated callus formation, and enhanced bone healing, confirming our hypothesis. Strategies to treat bone defects, fractures, non-unions, and arthrodeses by facilitating systemic cell recruitment may be an alternative to traditional bone grafting techniques in which the defect site is directly exposed.

## Acknowledgments

This research was supported by the Ellenburg Chair in Surgery at Stanford University, 1R01AR055650-8 04 from the National Institute of Health, and the French Granting Agency E.F.M.C. No. 1.

## Disclosure Statement

No competing financial interests exist.

## References

1. Mahendra, A., and Maclean A.D. Available biological treatments for complex non-unions. *Injury* **38 Suppl 4**, S7, 2007.
2. Goulet, J.A., Senunas L.E., DeSilva G.L., and Greenfield M.L. Autogenous iliac crest bone graft. Complications and functional assessment. *Clin Orthop Relat Res* **339**, 76, 1997.
3. Weiss, L. Web watch. *Tissue Eng* **8**, 167, 2002.
4. Younger, E.M., and Chapman M.W. Morbidity at bone graft donor sites. *J Orthop Trauma* **3**, 192, 1989.
5. Gerstenfeld, L.C., Alkhiary Y.M., Krall E.A., *et al.* Three-dimensional reconstruction of fracture callus morphogenesis. *J Histochem Cytochem* **54**, 1215, 2006.
6. Marsell, R., and Einhorn T.A. The biology of fracture healing. *Injury* **42**, 551, 2011.
7. Phillips, A.M. Overview of the fracture healing cascade. *Injury* **36 Suppl 3**, S5, 2005.
8. Bielby, R., Jones E., and McGonagle D. The role of mesenchymal stem cells in maintenance and repair of bone. *Injury* **38 Suppl 1**, S26, 2007.
9. Granero-Molto, F., Weis J.A., Miga M.I., *et al.* Regenerative effects of transplanted mesenchymal stem cells in fracture healing. *Stem Cells* **27**, 1887, 2009.
10. Kitaori, T., Ito H., Schwarz E.M., *et al.* Stromal cell-derived factor 1/CXCR4 signaling is critical for the recruitment of mesenchymal stem cells to the fracture site during skeletal repair in a mouse model. *Arthritis Rheum* **60**, 813, 2009.
11. Eghbali-Fatourehchi, G.Z., Lamsam J., Fraser D., *et al.* Circulating osteoblast-lineage cells in humans. *N Engl J Med* **352**, 1959, 2005.
12. Khosla, S., and Eghbali-Fatourehchi G.Z. Circulating cells with osteogenic potential. *Ann N Y Acad Sci* **1068**, 489, 2006.
13. Matsumoto, T., Kuroda R., Mifune Y., *et al.* Circulating endothelial/skeletal progenitor cells for bone regeneration and healing. *Bone* **43**, 434, 2008.
14. Otsuru, S., Tamai K., Yamazaki T., *et al.* Circulating bone marrow-derived osteoblast progenitor cells are recruited to the bone-forming site by the CXCR4/stromal cell-derived factor-1 pathway. *Stem Cells (Dayton, Ohio)* **26**, 223, 2008.
15. Shinohara, K., Greenfield S., Pan H., *et al.* Stromal cell-derived factor-1 and monocyte chemotactic protein-3 improve recruitment of osteogenic cells into sites of musculoskeletal repair. *J Orthop Res* **29**, 1064, 2011.
16. Glass, G.E., Chan J.K., Freidin A., *et al.* TNF-alpha promotes fracture repair by augmenting the recruitment and differentiation of muscle-derived stromal cells. *Proc Natl Acad Sci U S A* **108**, 1585, 2011.
17. Wang, D., Christensen K., Chawla K., *et al.* Isolation and characterization of MC3T3-E1 preosteoblast subclones with distinct *in vitro* and *in vivo* differentiation/mineralization potential. *J Bone Miner Res* **14**, 893, 1999.
18. Quarles, L.D., Yohay D.A., Lever L.W., *et al.* Distinct proliferative and differentiated stages of murine MC3T3-E1 cells in culture: an *in vitro* model of osteoblast development. *J Bone Miner Res* **7**, 683, 1992.
19. Choi, J.Y., Lee B.H., Song K.B., *et al.* Expression patterns of bone-related proteins during osteoblastic differentiation in MC3T3-E1 cells. *J Cell Biochem* **61**, 609, 1996.
20. Akman, A.C., Seda Tigli R., Gumusderelioglu M., and Nohutcu R.M. Bone morphogenetic protein-6-loaded chitosan scaffolds enhance the osteoblastic characteristics of MC3T3-E1 cells. *Artif Organs* **34**, 65, 2010.

21. Mizuno, M., Kitafima T., Tomita M., and Kuboki Y. The osteoblastic MC3T3-E1 cells synthesized C-terminal propeptide of type I collagen, which promoted cell-attachment of osteoblasts. *Biochim Biophys Acta* **1310**, 97, 1996.
22. Arguello, F., Baggs R.B., and Frantz C.N. A murine model of experimental metastasis to bone and bone marrow. *Cancer Res* **48**, 6876, 1988.
23. Arguello, F., Furlanetto R.W., Baggs R.B., *et al.* Incidence and distribution of experimental metastases in mutant mice with defective organ microenvironments (genotypes Sl/Sld and W/Wv). *Cancer Res* **52**, 2304, 1992.
24. Zilber, S., Lee S.W., Smith R.L., *et al.* Analysis of bone mineral density and bone turnover in the presence of polymethylmethacrylate particles. *J Biomed Mater Res B Appl Biomater* **90**, 362, 2009.
25. Kumagai, K., Vasanji A., Drazba J.A., *et al.* Circulating cells with osteogenic potential are physiologically mobilized into the fracture healing site in the parabiotic mice model. *J Orthop Res* **26**, 165, 2008.
26. Devine, M.J., Mierisch C.M., Jang E., *et al.* Transplanted bone marrow cells localize to fracture callus in a mouse model. *J Orthop Res* **20**, 1232, 2002.
27. Shen, F.H., Visger J.M., Balian G., *et al.* Systemically administered mesenchymal stromal cells transduced with insulin-like growth factor-I localize to a fracture site and potentiate healing. *J Orthop Trauma* **16**, 651, 2002.
28. Hernigou, P., Poignard A., Manicom O., *et al.* The use of percutaneous autologous bone marrow transplantation in nonunion and avascular necrosis of bone. *J Bone Joint Surg Br Vol* **87**, 896, 2005.
29. Hernigou, P., Poignard A., Beaujean F., and Rouard H. Percutaneous autologous bone-marrow grafting for non-unions. Influence of the number and concentration of progenitor cells. *J Bone Joint Surg Am Vol* **87**, 1430, 2005.
30. Barnes, G.L., Kostenuik P.J., Gerstenfeld L.C., and Einhorn T.A. Growth factor regulation of fracture repair. *J Bone Miner Res* **14**, 1805, 1999.
31. Linkhart, T.A., Mohan S., and Baylink D.J. Growth factors for bone growth and repair: IGF, TGF beta and BMP. *Bone* **19**, 1S, 1996.
32. Lee, D.H., Park B.J., Lee M.S., *et al.* Chemotactic migration of human mesenchymal stem cells and MC3T3-E1 osteoblast-like cells induced by COS-7 cell line expressing rhBMP-7. *Tissue Eng* **12**, 1577, 2006.
33. Kon, T., Cho T.J., Aizawa T., *et al.* Expression of osteoprotegerin, receptor activator of NF-kappaB ligand (osteoprotegerin ligand) and related proinflammatory cytokines during fracture healing. *J Bone Miner Res* **16**, 1004, 2001.
34. Trippel, S.B. Potential role of insulinlike growth factors in fracture healing. *Clin Orthop Relat Res* **355 Suppl**, S301, 1998.
35. Kim, S.-K., Kwon J.-Y., and Nam T.-J. Involvement of ligand occupancy in Insulin-like growth factor-I (IGF-I) induced cell growth in osteoblast like MC3T3-E1 cells. *BioFactors (Oxford, England)* **29**, 187, 2007.
36. Sudo, H., Kodama H.A., Amagai Y., *et al.* *In vitro* differentiation and calcification in a new clonal osteogenic cell line derived from newborn mouse calvaria. *J Cell Biol* **96**, 191, 1983.

Address correspondence to:

Stuart B. Goodman, M.D., Ph.D.

Department of Orthopaedic Surgery

Stanford University Medical Center Outpatient Center

Stanford University

450 Broadway St., M/C 6342

Redwood City, CA 94063

E-mail: goodbone@stanford.edu

Received: September 27, 2011

Accepted: November 30, 2011

Online Publication Date: January 4, 2012